High-Accuracy, Compact Database of Narrow-Band *k*-Distributions for Water Vapor and Carbon Dioxide

Anquan Wang and Michael F. Modest [1]

Department of Mechanical Engineering,
Pennsylvania State University, University Park, PA 16802, USA

Abstract

An accurate and compact narrow-band *k*-distribution database has been constructed for water vapor and carbon dioxide from the HITEMP and CDSD-1000 spectroscopic databases. The systematic approach of *k*-distribution data generation and compaction, storage optimization and interpolation is discussed in this paper. The new database enables the user to obtain narrow-band, part-spectrum and full-spectrum *k*-distributions for inhomogeneous gas mixtures.

Key words: thermal radiation; absorption coefficient; molecular gas mixtures; *k*-distributions; quadrature

1 Introduction

Radiative heat transfer in gaseous media can be evaluated most accurately by the line-by-line (LBL) approach, but LBL calculations are extremely time intensive and require large computer resources, considering that the radiative transfer equation (RTE) needs to be solved at up to a million wavenumbers. Since radiation calculations tend to be only a small part of the overall task in most combustion problems, the LBL approach is impractical for such applications. An inspection of the spectral distribution of gaseous absorption coefficients shows that the oscillatory absorption coefficient has the same value *k* at many different wavenumbers even across a very small portion of spectrum (narrow band), across which blackbody intensity and other radiative properties remain essentially constant. Recognition of this fact has led to the reordering of the absorption coefficient across such small wavenumber intervals into a monotonic absorption coefficient distribution against normalized artificial wavenumber, which is much more efficiently integrated across the spectrum. This is known as the narrow-band *k*-distribution approach, and is essentially exact for homogeneous media[1,2].

Like all traditional narrow-band approaches, the *k*-distribution model also has difficulties dealing with inhomogeneous media. Two methods have been devised to address the nonhomogeneity problem: the scaling approximation and the correlated-*k* assumption[3]. The former demands that spectral

---

[1] To whom all correspondence should be addressed. Fax: (814) 863-8682; Email: mfm6@psu.edu

and spatial dependence of absorption coefficient can be separated, which is somewhat more restrictive than the latter one, which only assumes that all wavenumbers that have the same absorption coefficient value k at one state also have always the same–but different–absorption coefficient value k^* at another state. This implies that, for a correlated absorption coefficient, the ratio k^*/k is an arbitrary function of k (but not wavenumber η) and space while, for a scaled absorption coefficient, the ratio k^*/k is a function of spatial location only. The correlated-k method has achieved great success in the field of meteorology, in which temperatures are low and change only slightly, while pressure changes can be very substantial[1,4,5]. In contrast, significant variations of temperature and concentration are common in combustion problems. Rivieŕe et al. have reported that the correlation of absorption coefficients breaks down in the presence of significant temperature gradients[6–8], since different spectral lines dominate radiative transfer at different temperatures. Similarly, in gas mixtures with strong changes in concentration, which also makes different spectral lines dominant in different locations, the correlatedness breakes down, as recognized by Modest and Zhang[9].

The reordering concept was first, in a coarse way, applied to the full spectrum by Denison and Webb[10,11]. They utilized the HITRAN spectroscopic database to calculate the weight factors for the popular Weighted-Sum-of-Gray-Gases (WSGG) method[12,13], calling it the Spectral-Line-Based WSGG (SLW) model; for nonhomogeneous gases they assumed a correlated absorption coefficient. Similarly, the related absorption distribution function (ADF) approach was developed by Riviére et al.[14,15]. Recently, Modest and Zhang[16] demonstrated that continuous k-distribution can also be obtained for the full spectrum, and revealed that the SLW/ADF/WSGG models are crude step implementations of their full-spectrum k-distribution (FSK) method. Also, Modest[9] provided a precise mathematical development of the correlated-k and scaled-k methods for narrow bands as well as for the full spectrum. For homogeneous media, FSK methods can achieve LBL accuracy at a tiny fraction of the computational cost, although substantial errors may occur when dealing with inhomogeneous media, since neither the scaled-k nor the correlated-k assumptions are ever truly accurate[3].

While FSK calculations are generally very accurate as well as efficient, they require knowledge of full-spectrum k-distributions, which are rather tedious to assemble from spectroscopic databases, such as HITRAN[17], HITEMP[18], and CDSD-1000[19]. Thus, to make FSK calculations feasible for general engineering use preassembled FSK distributions must be available from databases. Several approximate correlations have been generated by Denison and Webb[10,11,20,21] and by Modest et al.[3,9,22–25]. However, such correlations are of limited accuracy, and assembling mixture distributions from those for individual species has proven problematical (Solovjov and Webb[26]). Furthermore, adding nongray particle absorption backgrounds (such as soot) to FSK distributions is not possible. Very recently, Riazzi and Modest[27] developed a systematic approach to overcome these limitations by constructing full- and part-spectrum k-distributions for arbitrary mixtures from narrow-band k-distribution data. This makes it possible to obtain high-accuracy radiative transfer calculations of inhomogeneous gas-particulate mixtures at a reasonable computational cost, using precalculated sets of k-distributions.

It is the purpose of the present article to compile a highly accurate and compact database of narrow-band k-distributions for the most important combustion gases, from which high-accuracy full-spectrum k-distributions can be obtained efficiently for arbitrary mixtures of combustion gases, including nongray absorbing and/or scattering particles. Currently, water vapor and carbon dioxide, the two major

products of hydrocarbon–air combustion, are included in the database. The spectral absorption co-efficients for water vapor were calculated from HITEMP 2000[18], while for carbon dioxide CDSD-1000[19] was employed, which is considered more reliable than HITEMP for temperatures higher than 1000K[28, 29].

2 k-Distribution Generation

As stated earlier, it is the purpose of this work to collect an accurate and compact database of narrow-band k-distributions, from which full-spectrum k-distributions can be assembled for any total pressure (p), temperature (T) and mole fraction (x) of water vapor and carbon dioxide. Narrow-band k-distributions can be formulated mathematically as[30],

$$f(k) = \frac{1}{\Delta\eta} \int_{\Delta\eta} \delta(k - \kappa_\eta)d\eta, \tag{1}$$

and

$$g(k) = \int_0^k f(k')dk', \tag{2}$$

where η is the wavenumber, κ_η is the absorption coefficient calculated from a spectroscopic database, $\Delta\eta$ is the narrow-band width, $\delta(k)$ is the Dirac-delta function, $f(k)$ is the probability density function of the absorption coefficient value k (k-distribution), and $g(k)$ is the normalized artificial wavenumber (cumulative k-distribution). Through this reordering process, the absorption coefficient variable k becomes a monotonically increasing function of g.

Since k-distributions are generated from absorption coefficients, the underlying absorption coefficient data must be accurate, i.e., κ_η must be evaluated from spectroscopic databases at close enough spectral intervals to describe the irregularity of the absorption coefficient across the spectrum. At low pressures, line-broadening is relatively weak, causing little overlap between lines; at high pressures, on the other hand, line-broadening is strong, resulting in a smoother absorption coefficient. Therefore, the wavenumber resolution for low pressure calculations must be higher than for high pressures. In our work, a constant spacing across the entire spectrum was used; the resolution was considered sufficient if, when doubling the resolution, the error of narrow-band mean absorption coefficients stayed below 0.5 percent in major absorption bands of the entire spectrum. For instance, the required resolution for $p = 0.1$ bar was found to be 0.005 cm^{-1}, while 0.01 cm^{-1} was needed for $p = 1.0$ bar; both at $T = 1000$ K and $x = 1.0$. Similarly, high temperatures cause more line overlap than low temperatures, which would make the absorption coefficient distribution smoother. However, as temperature rises, "hot" lines become important, making the absorption coefficient distribution even more irregular. The combined effects lead to a need for high resolution at high temperatures. For example, for $p = 0.1$ bar and $x = 0.25$, the required resolution for 300 K was found to be 0.01 cm^{-1}, while 0.002 cm^{-1} was needed for 1000 K and 0.001 cm^{-1} for 2000 K.

In common industrial boilers and combustors as well as gas turbines, working conditions range from ambient to fairly high pressures, say 20–30 bar, while in rocket nozzles and closed-cycle gas turbines subatmospheric pressures may be encountered. Therefore, in the present database a large range of

3

Table 1
Precalculated gas states and narrow bands

Parameter	Sampling		Number of Samples
Species	CO_2, H_2O		2
Pressure (bar)	0.1 – 0.5:	every 0.1	5
	0.7:		1
	1.0 – 14.0:	every 1.0	14
	15.0 – 30.0:	every 5.0	4
	total:		24
Temperature (K)	300 – 2500: every 100		23
Mole Fraction	0.0 – 1.0 : every 0.25		5
Narrow Band (cm^{-1})	200 – 300:	every 10	10
	300 – 4000:	every 25	148
	4000 – 5000:	every 50	20
	5000 – 10000:	every 100	50
	10000 – 15000:	every 250	20
	total:		248

pressures ranging from as low as 0.1 bar to as high as 30 bar was considered, and a temperature range from 300 K to 2500 K. Higher temperatures appear meaningless because of the limitations of available spectroscopic databases. The mole fraction affects the (pressure-based) absorption coefficient only slightly through molecular size on collision broadening. Thus, only 5 mole fractions were considered here. The narrow-band division here is slightly different from that of Riazzi and Modest[27] in order to satisfy our accuracy requirements. Table 1 summarizes the pressures, temperatures, mole fractions and narrow bands stored in the present database.

When employing Eqs. (1) and (2) to calculate narrow-band cumulative k-distributions, a set of nominal k-values between the local maximum and minimum k-values must be chosen for each narrow band at the local gas state. Here we have used the distribution,

$$\Delta(k^\beta) = \left[(k_{max})^\beta - (k_{min})^\beta\right]/(N_{pt} - 1), \tag{3}$$

$$k_i = \left[(k_{min})^\beta + i\Delta(k^\beta)\right]^{1/\beta}, \quad i = 1, 2, ..., N_{pt}. \tag{4}$$

This power distribution of k-values employs an exponential factor β to generate a skewed distribution that places more points at smaller k-values than a linear distribution, but fewer than a logarithmic distribution. In the present work with $\beta = 0.1$ and a number of points $N_{pt} = 5000$, the recovered narrow band mean absorption coefficients compare to better than 0.01% with those from LBL calculations. Therefore, our k-distributions obtained from LBL data can be regarded as essentially error-free.

3   Data Compaction

While the 5000-point k-distributions have extremely high accuracy, for a database including 24 total pressures, 23 temperatures and 5 mole fractions for each of the two species, with the entire spectrum divided into 248 narrow bands, the resulting data would require 50 GB of storage. Obviously, such a huge database is not acceptable for practical calculations. Therefore, an efficient way needs to be found to compact these data into much smaller size while, at the same time, maintaining high accuracy. In the present database, during data compression, the accuracy of a k-distribution was determined (a) by comparing narrow-band averaged absorption coefficients with those obtained from LBL calculations, and (b) by comparing narrow-band gas column emissivities with LBL calculations (at a nominal optical thickness resulting in an emissivity of approximately 0.6). Accuracy was deemed acceptable if the errors stayed below 0.5%.

3.1   Fixed-g Concept

Each of the original cumulative k-distributions has a series of k-values (5,000 chosen values) and a corresponding series of 5000 g-values. If one series is fixed to be the same for all narrow bands, only the other series needs to be stored in the database. Since g always varies between 0 and 1, while the k-range varies dramatically from narrow band to narrow band, fixing the g-values is a logical choice. Since k-distributions are calculated for a chosen set of k-values, this requires inversion of the distribution through high-order interpolation, to obtain the corresponding set of k-values for a fixed set of g-values.

3.2   Quadrature Scheme

The set of g values needs to be chosen carefully, since it will directly affect the compression rate for the prescribed accuracy. Since n-node Gaussian quadrature has an $(2n - 1)$-th order of accuracy, the highest among present integration schemes, we chose the fixed-g series to be the abscissas of a certain Gaussian quadrature. In addition, we imposed two requirements for the desired quadrature scheme: (a) more points toward large g-values (corresponding to large k-values), since it is the larger k-values that tend to dominate radiative heat transfer rates, and (b) scalability, so that a lower rank quadrature is a subset of the next higher rank quadrature. With this feature one can use fewer points to perform a rough calculation, or use all the points in the database to obtain the highest accuracy.

The abscissas of a Gaussian quadrature between the limits of -1 and $+1$ are zeroes of a certain orthogonal polynomial. For the n-th rank Chebyshev polynomial of the second kind $U_n(x)$, the zeroes are[31],

$$x_n^k = \cos \theta_k, \quad k = 1, 2, ..., n, \tag{5}$$

and the corresponding Gaussian weight functions are

$$w_n^k = \frac{4 \sin \theta_k}{n + 1} \sum_{l=1}^{[(n+1)/2]} \frac{\sin(2l - 1)\theta_k}{2l - 1}, \tag{6}$$

5

where

$$\theta_k = \frac{k\pi}{n+1}.$$

Rearranging, it is observed that

$$x_n^k = \cos\left[\frac{2k\pi}{(2n+1)+1}\right] = x_{2n+1}^{2k} \equiv x_m^{2k}. \tag{7}$$

This implies that, for any given U_n, one can always find another U_m whose zeroes include all the zeroes of U_n, namely $m = 2n + 1$. The zeroes for every quadrature are distributed between $[-1, 1]$, and are symmetric around 0. In the present work, we are interested in quadrature over the range of g-values, i.e., between the limits of 0 and $+1$. Thus, for an arbitrary U_m, eliminating negative zeroes ($k > \lfloor m/2 \rfloor$), one obtains two possible quadrature schemes, viz.,

(I): Even-rank U_m, i.e., $m = 2n$.   ($n = 1, 2, 3, \ldots$)
The non-negative zeroes (quadrature points) can be rewritten as

$$x_n^k = \cos\theta_k, \quad k = 1, 2, ..., n, \tag{8}$$

where

$$\theta_k = \frac{k\pi}{2n+1}. \tag{9}$$

For the half-range quadrature, the weights are doubled, or

$$w_n^k = \frac{8\sin\theta_k}{2n+1} \sum_{l=1}^{n} \frac{\sin(2l-1)\theta_k}{2l-1}. \tag{10}$$

(II): Odd-rank U_m, i.e., $m = 2n - 1$.   ($n = 1, 2, 3, \ldots$)
The non-negative zeroes (quadrature points) can be rewritten as

$$x_n^k = \cos\theta_k, \quad k = 1, 2, ..., n, \tag{11}$$

where

$$\theta_k = \frac{k\pi}{2n} \tag{12}$$

Again, the weights are doubled, except for $k = n$, or

$$w_n^k = \frac{2(2 - \delta_{kn})\sin\theta_k}{n} \sum_{l=1}^{n} \frac{\sin(2l-1)\theta_k}{2l-1}, \tag{13}$$

where δ_{kn} is Kronecker's delta.

The advantage of quadrature (I) is that it has two open ends (i.e., excludes $x = 0, 1$), while quadrature (II) is open at one end ($x = 1$) but closed at the other ($x = 0$). The quadrature point at $x = 0$ (corresponding to $g = 0$ with the minimum k-value) is not very useful in k-distribution calculations. Because of this advantage, quadrature (I) will be used to present the final results of assembling full-spectrum k-distributions. On the other hand, quadrature (II) has better scalability which makes it
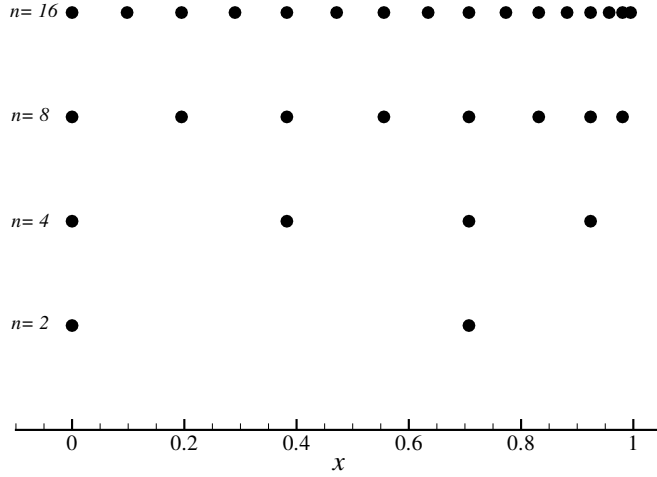
Fig. 1. Abscissa distributions of nested quadratures of scheme (II).

more ideal for data compaction than quadrature (I). The nesting relations of quadratures (I) and (II) are as follows.

$$(I): \quad x_n^k = x_{3n+1}^{3k}, \tag{14}$$
$$(II): \quad x_n^k = x_{2n}^{2k}. \tag{15}$$

In quadrature (II), the number of points (N_{pt}) grows much more slowly, allowing more nested ranks within a certain N_{pt} limit. If N_{pt} starts at $N_{pt} = 2$, then a series of 2^n is generated. Figure 1 shows this series of nested quadratures.

It is apparent that this quadrature puts more points toward the higher end, with roughly 25% of all points above $x = 0.9$. In some situations, one may need even more quadrature points near $x = 1$. In that case, a transformation may be employed, viz.,

$$x_n' = 1 - (1 - x_n)^\alpha,$$
$$w_n' = \alpha w_n (1 - x_n)^{\alpha-1}. \tag{16}$$

For example, with $\alpha = 3/2$, about 50% of all quadrature points are above $x = 0.9$. With quadrature (II) or its transformation, for each narrow-band cumulative k-distribution, using cubic spline interpolation at the quadrature abscissas, one can obtain a very compact substitute for the original distribution, subject to the 0.5% error limit mentioned earlier.

3.3 Database Structure

Using data compaction the original database was shrunk from 50 GB to 110 MB. This is still large enough to cause a bottleneck during calculations, unless fast data access methods are employed.

7

There are two kinds of data access methods for computer files, i.e., the sequential-access method and the direct-access method. In sequential format, the computer reads data in sequential manner, i.e., all data before the target data must be read also. The advantage of this method is that records can be of different lengths. On the other hand, it is apparent that it is not suitable in cases where small amounts of data, such as a compact k-series, are accessed frequently and randomly. The direct-access approach can avoid the above drawback. When performing I/O on a direct-access file, records can be read or written in any order. Its drawback is that the records must all be of the same length, while the lengths of compact k-series vary with total pressure, temperature, mole fraction, narrow band number and species. If each compact k-series was stored in one record, most records would contain lots of blanks and, thus, the method would be inefficient in terms of storage space.

A better approach, the approach taken in the present database, is to utilize the direct-access method while combining short k-series to fill the blanks in the records. If quadrature (II) is employed in data compaction, this combination is more efficient and easy to implement, since all compact k-distributions contain $N_{pt} = 2^n$ values. The combined lengths of two 16-point k-series are equal to the length of one 32-point k-series, etc. In this approach, an additional index file is required to record the locations of the k-series in the database file.

4   Interpolation on the Database

To obtain a narrow-band cumulative k-distribution for an arbitrary state, one needs to interpolate between precalculated states stored in the database. For a single specie, a narrow-band k-distribution is specified by its total pressure (p), temperature (T), mole fraction (x) and narrow band number. Thus, for a given narrow band, a three-dimensional interpolation in (p, T, x) is required, with precalculated (p,T,x) groups forming a grid in 3-D p-T-x space. Interpolation of cumulative k-distributions consists of interpolating the corresponding k-values for each fixed-g value. Therefore, all k-distributions involved must have the same fixed-g series. Since, as the result of data compaction, different k-distributions may have different N_{pt}, this may require an additional interpolation within individual k-distributions using, for instance, cubic spline interpolation.

The simplest and fastest 3-D interpolation scheme is trilinear interpolation, which employs a $2 \times 2 \times 2$ interpolation domain, although its accuracy may not always be satisfactory. Tricubic spline interpolation is a high-order scheme using polynomials with continuous 2nd-order derivatives. It can be shown that such polynomials exist and are unique[32]. To construct them, the smallest interpolation domain is $4 \times 4 \times 4$. To achieve small computational cost combined with acceptable accuracy, a hybrid scheme may be employed such as a 1-D spline interpolation in T and a 2-D bilinear interpolation in (p, x). Usually, one applies spline interpolation in those dimensions that are the major cause for error.

Figures 2 and 3 compare the narrow-band mean absorption coefficient and emissivity results obtained from the databased k-distributions with those from LBL calculations, at $p = 2.5$ bar, $T = 1550$ K and $x = 0.1$. The k-distributions were obtained by hybrid interpolation (cubic spline interpolation in T, bilinear interpolation in p and x) from the database. For H_2O, the mean absorption coefficient curve varies more smoothly and the errors are around or less than 1 percent for all narrow bands.
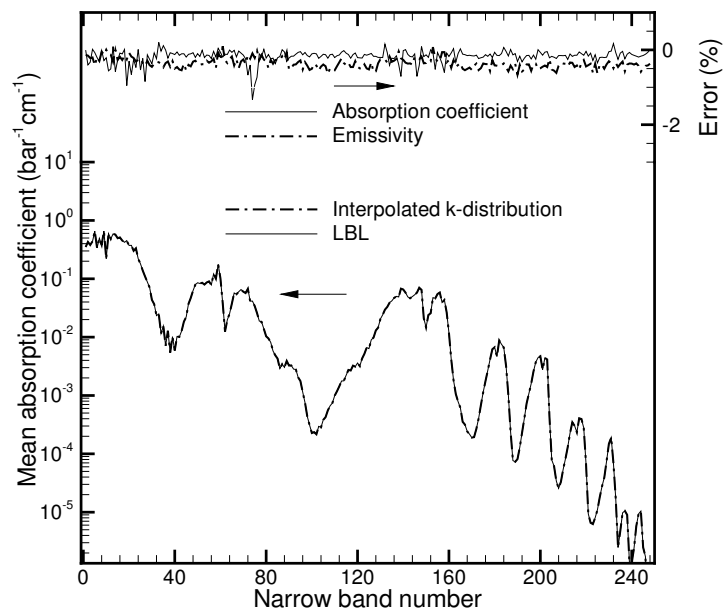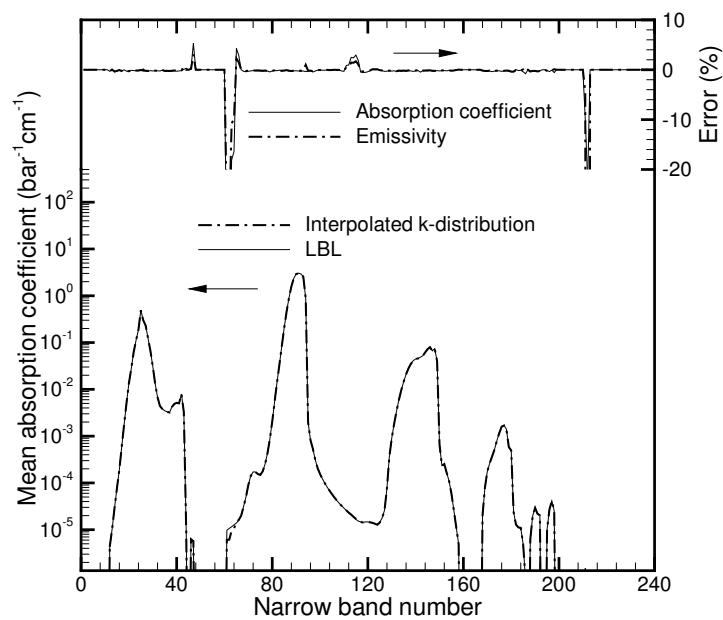
8

Fig. 2. Narrow-band mean absorption coefficient and emissivity obtained from interpolated k-distributions compared with LBL calculations; species: H_2O, $p = 2.5$ bar, $T = 1550$ K, $x = 0.1$; interpolation: hybrid.

Fig. 3. Narrow-band mean absorption coefficient and emissivity obtained from interpolated k-distributions compared with LBL calculations; species: CO_2, $p = 2.5$ bar, $T = 1550$ K, $x = 0.1$; interpolation: hybrid.

9

The absorption coefficient of CO_2 has more sharply pronounced bands, resulting in steep gradients, which may cause large errors. However, large errors are found to occur only for several unimportant narrow bands.

5 Full-Spectrum k-Distribution for Mixture

According to Modest[3], the Planck-function-weighted full-spectrum k-distributions are defined as

$$f(T, \underline{\phi}_0, k) = \frac{1}{I_b} \int_0^\infty I_{b\eta} \delta \left(k - \kappa_\eta(\underline{\phi}_0, \eta) \right) d\eta, \tag{17}$$

and

$$g(T, \underline{\phi}_0, k) = \int_0^k f(T, \underline{\phi}_0, k) dk = \int_0^{k^*} f(T, \underline{\phi}, k^*) dk^* = g(T, \underline{\phi}, k^*), \tag{18}$$

where $I_{b\eta}$ is the Planck function, $\underline{\phi}$ is the local state variable vector, i.e., $\underline{\phi} = (p, T, x)$, and $\kappa_\eta(\underline{\phi}_0, \eta)$ is the spectral absorption coefficient evaluated at a reference state $\underline{\phi}_0$. Eq. (18) implies a correlation of k and k^* between states $\underline{\phi}_0$ and $\underline{\phi}$. The reordered radiative transfer equation (RTE) becomes[3, 9]

$$\frac{dI_g}{ds} = k^*(T_0, \underline{\phi}, g) \left[a(T, T_0, g) I_b(T) - I_g \right] - \sigma_s(\underline{\phi}_s) \left[I_g - \frac{1}{4\pi} \int_{4\pi} I_g(\hat{s}') \Phi(\underline{\phi}_s, \hat{s}, \hat{s}') d\Omega' \right], \tag{19}$$

where

$$I_g = \int_0^\infty I_\eta \delta \left(k - \kappa_\eta(\underline{\phi}_0, \eta) \right) d\eta \Big/ f(T_0, \underline{\phi}_0, k), \tag{20}$$

$$a(T, T_0, g) = f(T, \underline{\phi}, k) \Big/ f(T_0, \underline{\phi}_0, k), \tag{21}$$

and $k^*(T_0, \underline{\phi}, g)$ is the k–g distribution, as given by Eq. (18), with the absorption coefficient evaluated at the local conditions $\underline{\phi}$ and the Planck function at the reference temperature T_0. Once the RTE is solved, the spectrally integrated intensity follows as[3]

$$I = \int_0^1 I_g dg. \tag{22}$$

The full-spectrum k-distributions given by Eq. (17) and Eq. (18) can be calculated directly from spectroscopic databases. However, Riazzi and Modest[27] demonstrated that the full-spectrum distributions can be more efficiently assembled from narrow-band distributions as

$$f(T, \underline{\phi}_0, k) = \sum_{j \in [\text{all NB's}]} \frac{I_{bj}}{I_b} f_j(\underline{\phi}_0, k), \tag{23}$$

and

$$g(T, \underline{\phi}_0, k) = \sum_{j \in [\text{all NB's}]} \frac{I_{bj}}{I_b} g_j(\underline{\phi}_0, k), \tag{24}$$

where

$$I_{bj} = \int_{\Delta\eta_j} I_{b\eta}(T)d\eta \tag{25}$$

is the Planck function integrated over narrow band $\Delta\eta_j$. Furthermore, they found that, for gas mixtures, the FSK may be obtained accurately from narrow-band k-distributions of the individual species. According to Riazzi and Modest[27], for a gas mixture of I species with uncorrelated absorption lines, the narrow band mixture k-distribution can be assembled from the individual species as,

$$g_{mix}(k_{mix}) = \int_{g_1=0}^{1} ... \int_{g_I=0}^{1} H\left[k_{mix} - (k_1 + ... + k_I)\right] dg_I...dg_1, \tag{26}$$

where H is the Heaviside step function. For a mixture of two species ($I = 2$), one may derive a more efficient relation as[27],

$$g_{mix}(k_{mix}) = \int_{0}^{1} g_2(k_{mix} - k_1)dg_1. \tag{27}$$

While Eqs. (26) and (27) can be applied equally to full-spectrum distributions, Riazzi and Modest[27] found that mixing H_2O and CO_2 on a narrow-band basis resulted in virtually no error, whereas full-spectrum mixing generally produced small errors (of a few percent). Furthermore, using narrow-band k-distributions allows for easy mixing with nongray absorbing particles: after obtaining the narrow-band k-distributions for the gas mixture, the (for each narrow band constant) particle absorption coefficient is simply added before assembling the full-spectrum k-distribution. Figure 4 shows a comparison between full-spectrum k-distributions assembled from the narrow-band database and those calculated directly from the spectroscopic databases for a 10% CO_2-20% H_2O-70% N_2 gas mixture at $p = 2.5$ bar and $T = 1550$ K . Also shown is the FSK for the same gas mixture also containing a volume fraction $f_v = 10^{-7}$ of nongray soot. The soot's complex index of refraction, $m = n - ik$, was modelled using the correlations developed by Chang and Charalampopoulos[30, 33],

$$n = 1.811 + .1263\ln\lambda + .0270\ln^2\lambda + .0417\ln^3\lambda, \tag{28}$$

$$k = .5821 + .1213\ln\lambda + .2309\ln^2\lambda - .0100\ln^3\lambda, \tag{29}$$

where λ is the wavelength in μm, valid over the wavelength range [0.4μm, 30μm]. The soot's absorption coefficient was determined using the small particle limit of Rayleigh scattering for a cloud of non-uniform particles given by[30]

$$\kappa_\lambda = \frac{36\pi nk}{(n^2 - k^2 + 2)^2 + 4n^2k^2}\frac{f_v}{\lambda}. \tag{30}$$

As shown in Figure 4, there is no distinguishable difference between the full-spectrum k-distribution compiled from the narrow-band database and the one calculated directly from the spectroscopic databases, for both the gas mixture as well as the one containing soot, except that the FSK's assembled from the narrow-band database, employing quadrature (I) which is open at both ends (does not include $g = 0$ and $g = 1$), cannot include the minimum and maximum k-values .
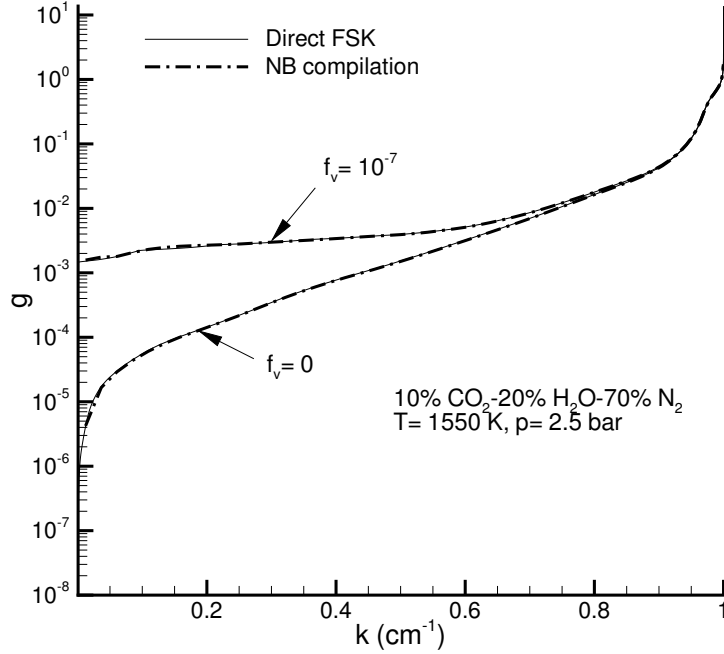
11

Fig. 4. Full-spectrum k-distributions assembled from the narrow band database.

6   Sample Calculations

To test the accuracy of the new database, a large number of heat transfer calculations were carried out for one-dimensional slabs of homogeneous gas mixtures bounded by cold black walls. Such problems produce "exact" results if "exact" k-distributions are employed; any error, therefore, is due to inaccuracies in the assembly of the k-distribution. In all cases, a 20% H_2O–10% CO_2–70% N_2 (in volume) mixture with or without soot was considered, for which the local radiative heat source, dq/dx, was calculated in non-dimensional fashion as

$$\left(\frac{dq}{dx}\right)_{\text{normalized}} = \frac{dq/dx}{\sigma T^4/L},\tag{31}$$

where T is the temperature and L is the thickness of the slab. Effects of varying total pressure, temperature, thickness and amount of soot were investigated as summarized in Table 2. All FSK calculations employed a 10-point quadrature of type (I) and, in most cases, the maximum error across the slab stayed around or below 2%. Exceptions occurred only at fairly small optical thicknesses, which will be discussed in more detail later in this section.

Figures 5 through 8 show the representative curves of normalized dq/dx across the slab. For better readibility, only LBL results and errors made by database-assembled k-distribution calculations were plotted. Figure 5 shows the effects of total pressure on overall accuracy, keeping all other parameters fixed. For low pressures such as 0.25 bar, dq/dx is essentially constant across the slab, since the gas is so optically thin that all emission escapes from the medium without self-absorption. As pressure

12

Table 2
Investigated gas/particulate mixture states

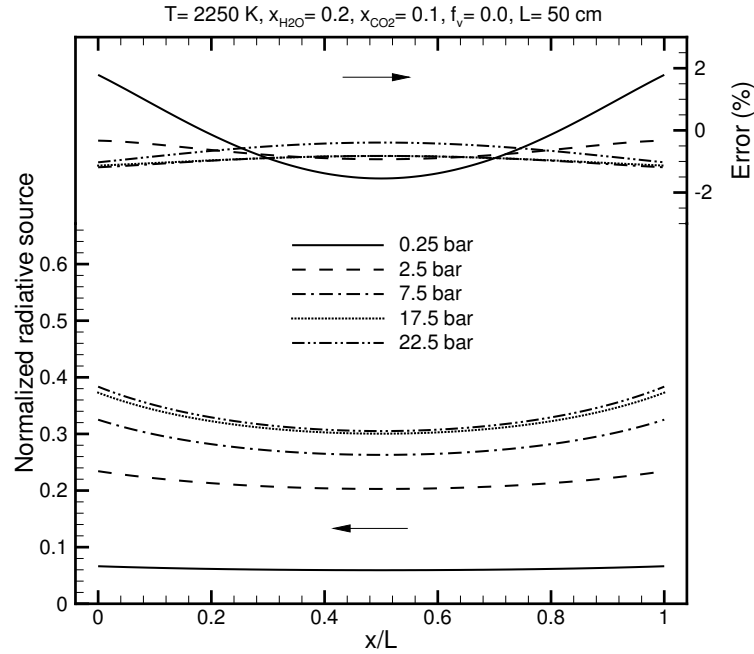|	
p (bar)	0.25, 0.85, 2.5, 7.5, 17.5, 22.5
T (K)	450, 750, 1250, 1750, 2250
L (cm)	0.1, 1.0, 10.0, 50.0, 100.0
f_v	0.0, 10^{-8}, 10^{-7}, 10^{-6}

Fig. 5. Normalized radiative source for a 20% H_2O–10% CO_2–70% N_2 mixture at varying pressures; $T = 2250$ K, $f_v = 0.0$, $L = 50$ cm; 10-point quadrature (I).

rises, the gas becomes optically thicker and, therefore, energy emitted near the center cannot escape, leading to strong gradients toward the boundaries. The same phenomenon can be seen in Figure 6, in which the soot volume fraction f_v is increased, and in Figure 8, in which the slab width L is increased, both causing the mixture to become more opaque. In Figure 7 only temperature T is varied, causing the Planck function peak to shift from one absorption band to another. Therefore, in Figure 7, there is a specific temperature at which the gas is the most opaque.

In Figure 8, one can observe a large error at the smallest thickness of $L = 0.1$ cm. At this thickness, the gas is optically extremely thin, putting all importance on the large k-values. The large error implies that an insufficient number of quadrature points has been placed on high g-values, which correspond to large k-values. In order to decrease the error, one may use the quadrature transformation discussed earlier, to put enough quadrature points on high g-values (increasing the transformation factor α). As shown in Figure 9, without increasing the number of the quadrature points, using the quadrature transformation, the error was reduced to almost 0 with a value of $\alpha = 2.5$.

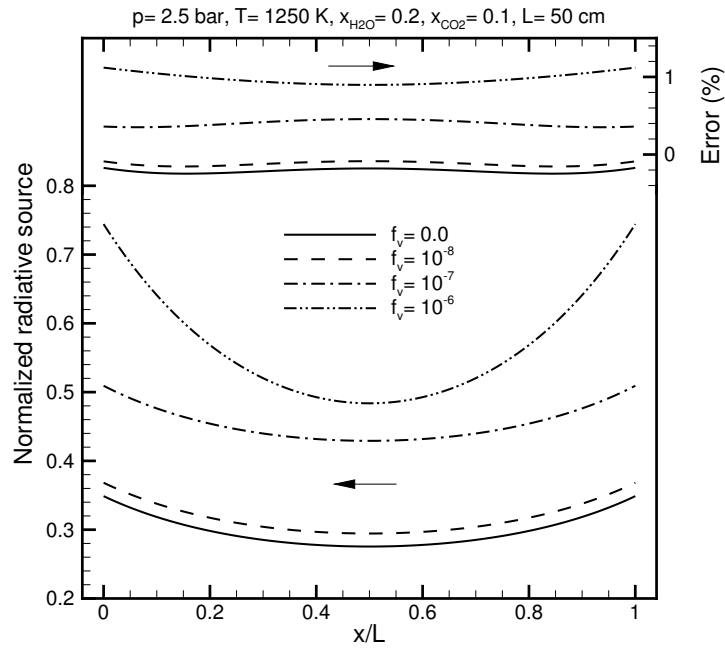In conclusion, we may state that the present narrow-band k-distribution database can be used to as-

13

Fig. 6. Normalized radiative source for a 20% H_2O–10% CO_2–70% N_2 mixture with varying soot concentrations; p = 2.5 bar, T = 1250 K, L = 50 cm; 10-point quadrature (I).
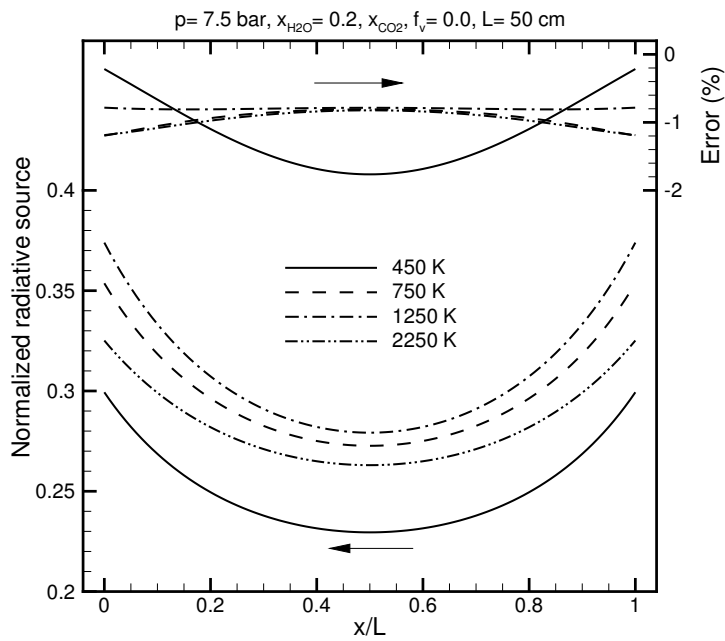

Fig. 7. Normalized radiative source for a 20% H_2O–10% CO_2–70% N_2 mixture at varying temperatures; p = 7.5 bar, f_v = 0.0, L = 50 cm; 10-point quadrature (I).
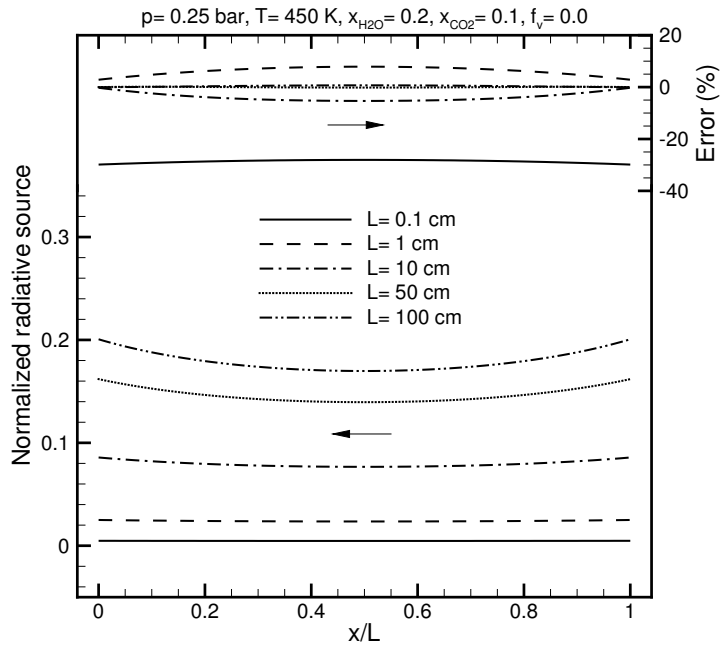
14

Fig. 8. Normalized radiative source for a 20% H_2O–10% CO_2–70% N_2 mixture at varying slab thicknesses; $p = 0.25$ bar, $T = 450$ K, $f_v = 0.0$; 10-point quadrature (I).
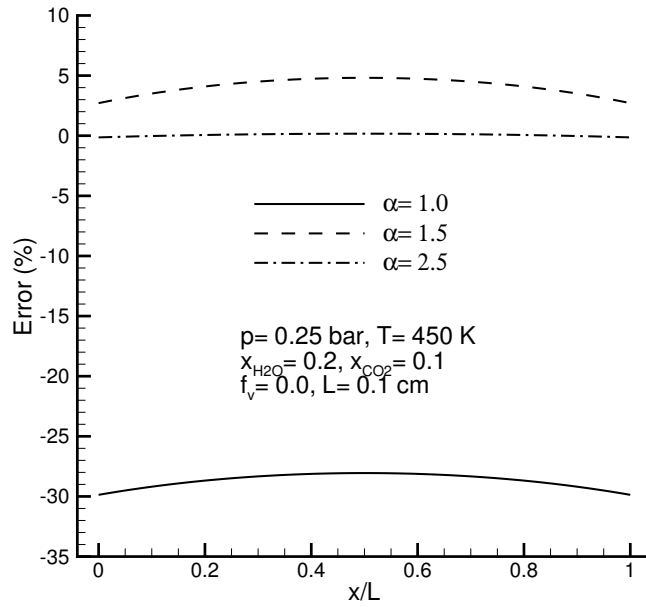

Fig. 9. Errors for different transformations of quadrature (I); $p = 0.25$ bar, $T = 450$ K, $f_v = 0.0$, $L = 0.1$ cm; 10-point quadrature.

semble small and accurate full-spectrum k-distributions, which, in turn, can produce high accuracy radiation calculations of gas/particulate mixtures, provided that an appropriate quadrature set is employed.

7 Summary

In this paper, an accurate and compact narrow-band k-distribution database has been constructed for water vapor and carbon dioxide. Using the same methods for narrow-band k-distribution generation, data compaction and storage optimization, the database can readily be extended to include other gases.

In order to obtain high-accuracy k-distributions, care was taken to first evaluate spectral absorption coefficients of high accuracy from spectroscopic databases. To compact a large amount of raw k-distribution data into a small, but accurate database and to achieve high accuracy in radiation calculations, a fixed-g concept was introduced. In addition, two requirements were imposed for the quadrature scheme employed in data compaction: (a) more quadrature points for large g-values (corresponding to large k-values, which tend to be more important), and (b) scalability, so that a lower rank quadrature is nested in the next higher rank quadrature, allowing users to choose the number of data points according to their own accuracy requirement. Two quadrature schemes (I) and (II) were developed to meet these two requirements. Quadrature (I) is open at its two boundaries (i.e., excludes $g = 0$ and $g = 1$), making it superior for radiation calculations, and was employed for the final full-spectrum k-distribution assembly. Quadrature (II) is open at one boundary ($g = 1$) and has better scalability than quadrature (I), making it ideal for data compression and database construction. Using quadrature (II) and its transformation, a large quantity of k-distribution data calculated from spectral data was successfully compacted into a database of small size while, at the same time, maintaining high accuracy.

It was demonstrated that single specie narrow-band k-distributions at arbitrary thermal states can be obtained accurately from the new database by an interpolation scheme presented in this paper. Furthermore, with the models developed by Riazzi and Modest[27], full-spectrum (or part-spectrum) k-distributions for inhomogeneous nongray gas/particulate mixtures can also be assembled accurately. Sample calculations investigating the effects of total pressure, temperature, optical thickness and soot concentration on the overall error of radiation calculations showed that, employing an appropriate quadrature set, full-spectrum k-distributions obtained from the new database provide highly accurate radiation results with very few quadrature points.

References

1. Lacis, A. A. and Oinas, V., A Description of the Correlated-k Distribution Method for Modeling Nongray Gaseous Absorption, Thermal Emission, and Multiple Scattering in Vertically Inhomogeneous Atmospheres, Journal of Geophysical Research 1991, 96(D5): 9027–9063.

2. Goody, R. M. and Yung, Y. L., *Atmospheric Radiation – Theoretical Basis*, Oxford University Press, New York 2nd edn. 1989.

3. Modest, M. F., Narrow-band and full-spectrum k-distributions for radiative heat transfer—correlated-k vs. scaling approximation, JQSRT 2003, 76(1): 69–83.

4. Goody, R., West, R., Chen, L., and Crisp, D., The Correlated-k Method for Radiation Calculations in Nonhomogeneous Atmospheres, JQSRT 1989, 42(6): 539–550.

5. Fu, Q. and Liou, K. N., On the Correlated k-Distribution Method for Radiative Transfer in Nonhomogeneous Atmospheres, J. Atm. Sci. 1992, 49(22): 2139–2156.

6. Rivière, P., Soufiani, A., and Taine, J., Correlated-k and Fictitious Gas Methods for H_2O near $2.7\,\mu$m, JQSRT 1992, 48: 187–203.

7. Rivière, P., Scutaru, D., Soufiani, A., and Taine, J., A New $c - k$ Data Base Suitable from 300 to 2500 K for Spectrally Correlated Radiative Transfer in CO_2–H_2O Transparent Gas Mixtures, in *Tenth International Heat Transfer Conference*, Taylor & Francis 1994: 129–134.

8. Rivière, P., Soufiani, A., and Taine, J., Correlated-k and fictitious gas model for H_2O infrared radiation in the Voigt regime, JQSRT 1995, 53: 335–346.

9. Modest, M. F. and Zhang, H., The Full-Spectrum Correlated-k Distribution For Thermal Radiation from Molecular Gas–Particulate Mixtures, ASME J. Heat Transfer 2002, 124(1): 30–38.

10. Denison, M. K. and Webb, B. W., A Spectral Line Based Weighted-Sum-of-Gray-gases Model for Arbitrary RTE Solvers, ASME J. Heat Transfer 1993, 115: 1004–1012.

11. Denison, M. K. and Webb, B. W., The Spectral-Line-Based Weighted-Sum-of-Gray-Gases Model in Nonisothermal Nonhomogeneous Media, ASME J. Heat Transfer 1995, 117: 359–365.

12. Hottel, H. C. and Sarofim, A. F., *Radiative Transfer*, McGraw-Hill, New York 1967.

13. Modest, M. F., The Weighted-Sum-of-Gray-Gases Model for Arbitrary Solution Methods in Radiative Transfer, ASME J. Heat Transfer 1991, 113(3): 650–656.

14. Rivière, P., Soufiani, A., Perrin, M. Y., Riad, H., and Gleizes, A., Air Mixture Radiative Property Modelling in the Temperature Range 10000–40000 K, JQSRT 1996, 56: 29–45.

15. Pierrot, L., Rivière, P., Soufiani, A., and Taine, J., A Fictitious-gas-based Absorption Distribution Function Global Model for Radiative Transfer in Hot Gases, JQSRT 1999, 62: 609–624.

16. Modest, M. F. and Zhang, H., The Full-Spectrum Correlated-k Distribution and its Relationship to the Weighted-Sum-of-Gray-Gases Method, in *Proceedings of the 2000 IMECE* HTD-366-1 Orlando, FL ASME 2000: 75–84.

17. Rothman, L. S. and many others, The HITRAN Spectroscopic Molecular Database: Edition of 2000 including updates through 2001, JQSRT 2003, 82(1–4): 5–44.

18. Rothman, L. S., Camy-Peyret, C., Flaud, J.-M., Gamache, R. R., Goldman, A., Goorvitch, D., Hawkins, R. L., Schroeder, J., Selby, J. E. A., and Wattson, R. B., HITEMP, the High-Temperature Molecular Spectroscopic Database 2000, available through `http://www.hitran.com`.

19. Tashkun, S. A., Perevalov, V. I., Bykov, A. D., Lavrentieva, N. N., and Teffo, J.-L., Carbon Dioxide Spectroscopic databank (CDSD), available from ftp://ftp.iao.ru/pub/CDSD-1000 2002.

20. Denison, M. K. and Webb, B. W., The Spectral-Line Weighted-Sum-of-Gray-Gases Model for H_2O/CO_2 Mixtures, ASME J. Heat Transfer 1995, 117: 788–792.

21. Denison, M. K. and Webb, B. W., The spectral line weighted-sum-of-gray-gases model—a review, in Mengüç, M. P., ed., *Proceedings of the First International Symposium on Radiation Transfer*, Begell House 1996: 193–208.

22. Zhang, H. and Modest, M. F., A Multi-Level Full-Spectrum Correlated-k Distribution For Ra-

diative Heat Transfer in Inhomogeneous Gas Mixtures, JQSRT 2002, 73(2–5): 349–360.

23. Zhang, H. and Modest, M. F., Full-Spectrum *k*-Distribution Correlations for Carbon Dioxide Mixtures, J. Thermoph. Heat Transfer 2003, 17(2): 259–263.

24. Zhang, H. and Modest, M. F., Scalable Multi-Group Full-Spectrum Correlated-*k* Distributions For Radiative Heat Transfer, ASME J. Heat Transfer 2003, 125(3): 454–461.

25. Zhang, H. and Modest, M. F., Multi-Group Full-Spectrum *k*-Distribution Database For Water Vapor Mixtures in Radiative Transfer Calculations, Intl. J. Heat Mass Transfer 2003, 46(19): 3593–3603.

26. Solovjov, V. and Webb, B. W., SLW Modeling of Radiative Transfer in Multicomponent Gas Mixtures, JQSRT 2000, 65: 655–672.

27. Riazzi, R. J. and Modest, M. F., Assembly of Full-Spectrum *k*-Distributions from a Narrow-Band Database; Effects of Mixing Gases, Gases and Nongray Absorbing Particles, and Mixtures with Nongray Scatterers in Nongray Enclosures, JQSRT 2004, in print.

28. Tashkun, S. A., Perevalov, V. I., Teffo, J.-L., Bykov, A. D., and Lavrentieva, N. N., CDSD-1000, the high-temperature carbon dioxide spectroscopic databank, JQSRT 2003, 82(1–4): 165–196.

29. Modest, M. F. and Bharadwaj, S. P., High-Resolution, High-Temperature Transmissivity Measurements and Correlations for Carbon Dioxide–Nitrogen Mixtures, JQSRT 2002, 73(2–5): 329–338.

30. Modest, M. F., *Radiative Heat Transfer*, Academic Press, New York 2nd edn. 2003.

31. Davis, P. J. and Rabinowitz, P., *Methods of Numerical Integration*, Academic Press Inc, Orlando 2nd edn. 1984.

32. Uciński, D., *Measurement Optimization for Parameter Estimation in Distributed Systems*, Technical University Press, Zielona Góra, Poland 1984.

33. Chang, H. and Charalampopoulos, T. T., Determination of the wavelength dependence of refractive indices of flame soot, Proceedings of the Royal Society (London) A 1990, 430(1880): 577–591.